doi:10.2533/chimia.2015.530 Chimia 69 (2015) 530–536

Synthetic G-Quartets as Versatile Nanotools for the Luminescent Detection of G-Quadruplexes

Aurelien Laguerre, Marine Levillain, Loic Stefan, Romain Haudecoeur, Fares Katranji, Marc Pirrotta, and David Monchaud*

Abstract: Recent years have witnessed a tremendous increase in the biotechnological applications of nucleic acid-based nanotools. Beyond their biological relevance, nucleobases have indeed found new scopes of applications in bionanotechnology, which are expanding nowadays at an accelerated pace. Among the four canonical nucleobases (adenine, guanine, cytosine and thymine), guanine is certainly the most useful and used base, thanks to its versatile H-bond donating/accepting properties that make it suitable for being involved in various assemblies ranging from base-pairs to base-quartets. Here, we would like to report on an innovative guanine-based molecular tool named Tb.Pyro-DOTASQ: this metal complex has a sophisticated chemical structure that allows formation of an intramolecular G-quartet upon interaction with alternative secondary structures known as G-quadruplexes. This target-promoted molecular switch triggers a luminescence response that would permit the use of Tb.Pyro-DOTASQ to search and detect quadruplex-forming DNA and RNA sequences: its unique design indeed allows it i) to create specific interaction with quadruplexes, ii) to provide an easily readable luminescent output to monitor this association and iii) to be readily immobilized on graphene surface, thus making Tb.Pyro-DOTASQ a high-value molecular device. Results obtained in the course of in-depth biophysical analyses raise questions about the actual supramolecular structure of Tb.Pyro-DOTASQ: these results thus shed a bright light on the care that must be exercised when using intricate molecular architectures to construct elaborated supramolecular metal complexes.

Keywords: DOTA · G-quadruplexes · Luminescence · Pyrene · TASQ · Terbium

Introduction

Only a few years after the elucidation of the DNA double helix structure by Watson and Crick (in 1953),[1] the first demonstrations describing the non-linear relationship between the nucleobase composition of short DNA strands and the stability of their secondary structures were reported. Notably, Sueoka, Marmur and Doty reported in 1959 that the density of guanine/cytosine-rich deoxyribonucleic acids was slightly higher than theoretically calculated: they wisely mused that this difference could originate in the folding of DNA in a more compact structure in which guanine and cytosine are improperly paired.[2] In 1962, Gellert, Lipsett and Davies demonstrated that higher-order gel-type nucleobase assemblies could be formed in concentrated solutions of guanylic acids.[3] In their model, the four guanines were linked *via* an array of eight Hoogsteen-type hydrogen bonds (H-bonds), forming planar macrocycles (so called G-tetramers, later known as G-quartet or G-tetrads) able to self-stack thanks to π-stacking interactions. These results were the first evidence that nucleobases, and beyond this, nucleic acids, could adopt transiently non-canonical supramolecular arrangements.

The ability of nucleobases (comprising two purines: adenine (A) and guanine (G), and two pyrimidines: cytosine (C) and thymine (T), Fig. 1A) to self-assemble originates in their capability to accept and donate H-bonds in a highly versatile manner.[4] The Watson-Crick base-pairing relies on three H-bonds in the GC pair and 2 H-bonds in the AT pair (Fig. 1B). This H-bond pattern, albeit iconic, does not fully exploit the donating/accepting potential of nucleobases: purines indeed display two to three donor/acceptor sites, while pyrimidines can donate/accept one to four H-bonds. This versatility allows nucleobases to form up to 28 distinct base-pairs involving at least two H-bonds.[4] This unique property, along with the non-covalent, reversible nature of H-bonds, explains why nucleobases have played and continue to play central roles in supramolecular chemistry.

Guanine is undoubtedly the most fascinating nucleobase. Its highly versatile H-bond creating capability (*i.e.* three donating and three accepting sites) makes it suited for participating in higher-order supramolecular assemblies whose nature mainly depends on the experimental conditions: they can be involved either in GC base pairs under classical Watson-Crick conditions (Fig. 1B), or in G-quartets (*i.e.* cyclic arrays of four G held together *via* eight Hoogsteen-type H-bonds, Fig. 1C) in cation-rich water solutions, and G-ribbons (*i.e.* linear and virtually infinite ribbon-like arrangements) in cation-less organic solvents.[5] The G-quartet is the most promising G-based nanotool, owing to its discrete (four guanines) and controllable (cation-dependent stability) and chemical nature (guanosines can be conveniently replaced by synthetic guanine derivatives). The biotechnological applications of G-quartets depend on their nature: i) intermolecular synthetic G-quartets (that is, G-quartets that result from the assembly of guanines belonging to two to four different partners) have been successfully used as building blocks for stable and tunable hydrogels,[6] artificial ionophores,[7] *etc.*; ii) intramolecular synthetic G-quartets (*i.e.* G-quartets that result from the association of four guanines present in the same scaffold) have been used as cation extractants,[8] pre-catalyst for pseudo-enzymatic reactions,[9] *etc.*; and iii) contrary to intermolecular

*Correspondence: Dr. D. Monchaud
Institute of Molecular Chemistry
University of Dijon
ICMUB CNRS UMR6302
Dijon, France
E-mail: david.monchaud@cnrs.fr

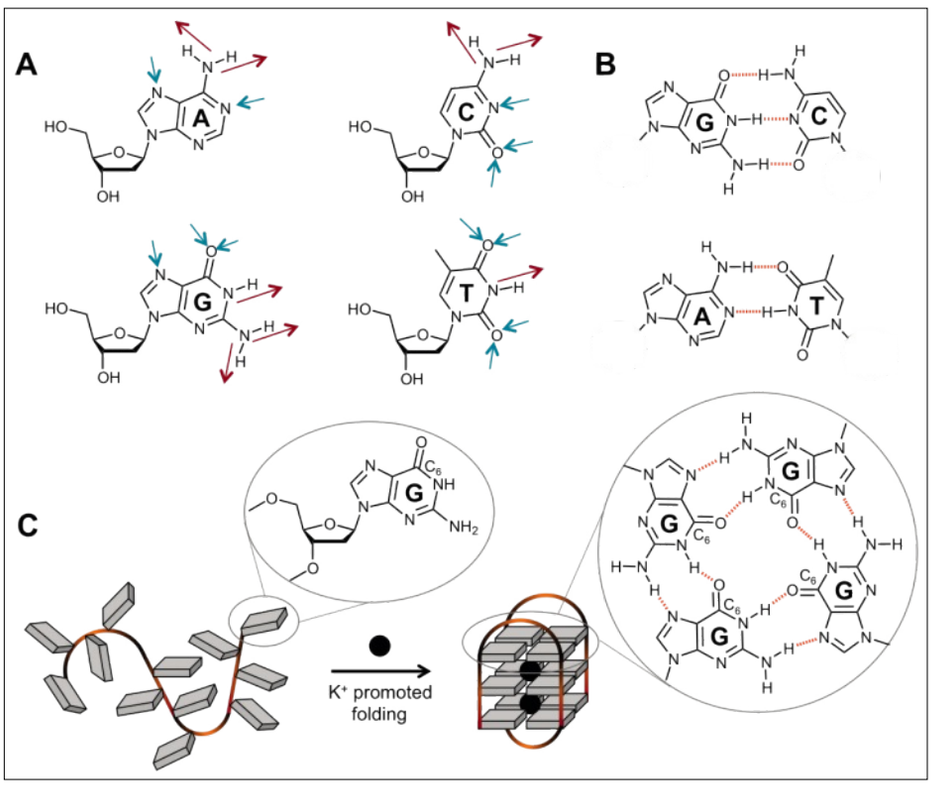

Fig. 1. Schematic representation of the nucleobases adenine (A), cytosine (C), guanine (G) and thymine (T), along with their donating (red arrow)/accepting (blue arrow) H-bond sites (**A**), of the GC and AT Watson-Crick base pairs (**B**), and of the intramolecular folding of a G-rich DNA sequence to form a quadruplex-DNA whose basic building block is a G-quartet (**C**).

native G-quartets (which have found only limited applications), intramolecular native G-quartets (that is, G-quartets that result from the assembly of guanosines of G-rich DNA/RNA strands, also known as G-quadruplexes) have found interesting applications, notably as quadruplex-based DNAzyme-type catalysis.[10] However, intramolecular native G-quartets (DNA and RNA quadruplexes) are above all intensively studied for their current biological relevance.[11]

G-quadruplexes (Fig. 1C) result from the ability of G-rich DNA and RNA sequences to fold into a secondary structure comprising stacks of two or more G-quartets stabilized by both π-stacking interactions (between the quartet planes) and chelation of physiologically relevant cations (in between the quartet planes).[12] Cations such as sodium or potassium are indeed intercalated in between the G-tetrads to avoid electrostatic repulsion of C_6-carbonyls that point towards the inner cavity of the quartet. Computational analysis has shown that more than 370,000 of putative G-quadruplex forming sequences were found *in silico* in the human genome.[13] Recent demonstrations of the existence of such a structure in human cells[14] have paved a very promising way to develop new anti-cancer strategies targeting DNA/RNA in a structure-specific rather than a sequence-selective manner. However, the discovery of more and more quadruplex-forming sequences in the human genome (in telomeres and promoters of oncogenes)[15] and transcriptome (in telomeric transcripts and regulatory regions of messenger RNA),[16] along with their high structural polymorphism, make their therapeutic relevance far more challenging than expected.[17]

To tackle the issue of the genome-wide analysis of quadruplexes *in cellulo*, various strategies have been recently implemented.[18] Among them, the pull-down approach offers both simplicity and efficiency. This method relies on immobilizable quadruplex-affinic compounds (quadruplex ligands) that interact with quadruplexes on one hand and allow the resulting quadruplex/ligand assemblies to be readily extracted from biofluids (cell extracts) *via* a surface-immobilization step on the other hand (Fig. 2). For this approach to be successful the ligands must display an equal affinity for quadruplexes whatever their topologies are (whatever the sequences they fold from). Our recent reports on the use of template assembled synthetic G-quartets (TASQ) as efficient and multi-target quadruplex ligands (*vide infra*)[19–21] demonstrated that they could be valuable tools for DNA pull-down strategies. However, this requires the introduction of an immobilizing appendage, which turns out to be rather chemically challenging. Herein, we would like to report on the design, the synthesis and preliminary *in vitro* evaluations of a new TASQ ligand that aims at being a versatile and multitasking tool dedicated to the detection of G-quadruplexes *in vitro*. Our objective is to structurally fine-tune one of our promising candidates, a luminescent light-up probe referred to as Tb.DOTASQ;[19] we selected this candidate (displaying neutral guanine arms)[19,20] since contrary to the TASQ recently developed (with cationic guanine arms)[14e,21] the terbium is mandatory to make the resulting metal complexes quadruplex-affinic ligands. Our aim is thus to deliver a new molecule able to act as graphene-immobilizable quadruplex ligand providing output luminescent signals to readily monitor quadruplex bindings.

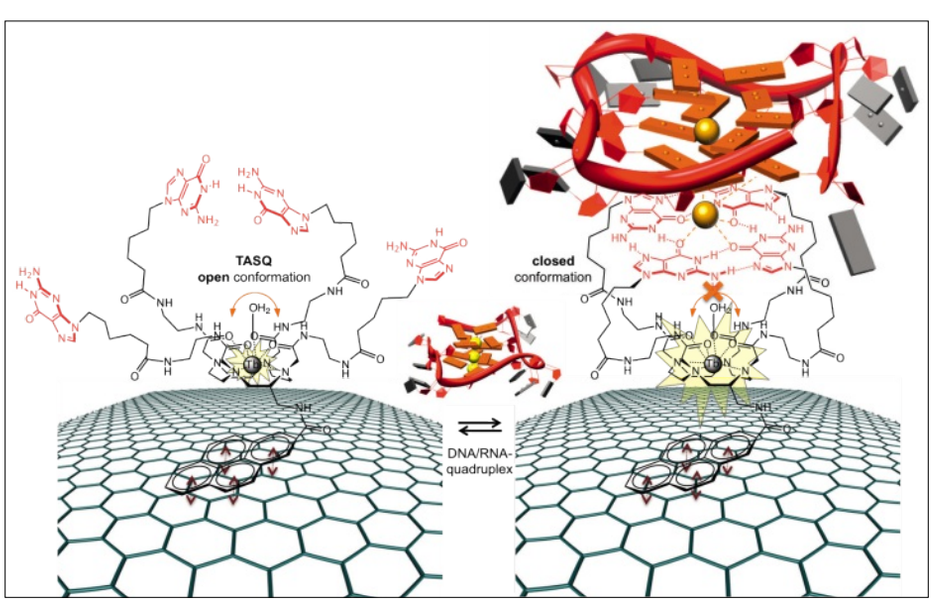

Fig. 2. Schematic representation of a pull-down strategy aiming at isolating and detecting quadruplexes *in vitro*: the terbium complex Tb.Pyro-DOTASQ enables both surface immobilization (*via* pyrene/graphene interaction) and detection of quadruplexes (*via* an enhancement of its luminescent properties).

Results and Discussion

Design of Tb.Pyro-DOTASQ

DOTASQ (for DOTA-templated Synthetic G-Quartet) represented the very first reported example of biomimetic quadruplex ligands.[19] The conception of this ligand was based on the observation that the stability of a quadruplex depends on the number of its constitutive tetrads (*i.e.* the more, the better). From this observation, we inferred that a synthetic quartet could be an excellent quadruplex ligand. Indeed, the interaction between the native quartet and the synthetic one occurred according to a nature-inspired process that is at the origin of quadruplex stability (π-stacking interactions plus cation chelation). DOTASQ exists under two distinct conformations (Fig. 2), an 'opened' one in which the four guanines are independent, and the 'closed' one in which the intramolecular G-quartet is folded. The latter conformation is required for binding to quadruplexes, a nature-inspired association driven by shape similarity between synthetic (ligand) and native (quadruplex) quartets. This '*like-likes-like*' recognition explains the high level of quadruplex selectivity of DOTASQ, since only shapes matter (that is, duplexes cannot trigger the DNA-affinic closed conformation). However, because of the too high conformational flexibility of the DOTA template, DOTASQ itself was found unable to interact efficiently with quadruplexes. We thus developed Tb.DOTASQ, the corresponding terbium complex of DOTASQ, to address this issue. The terbium ion brings a double dividend: on one hand, it favors the formation of the intramolecular G-quartet, blocking the DOTA in a conformation that directs the four guanine arms on the same side of the template. On the other hand, the terbium reports on the conformation of DOTASQ since its bound water molecule (the 9th coordination, Fig. 2) moves freely when the TASQ is in its open conformation (the luminescence is low) while its exchange rate is lowered when the TASQ adopts its closed conformation (the luminescence is high). Tb.DOTASQ displays a fair G-quadruplex affinity, as judged by FRET-melting assays,[22] with $\Delta T_{1/2} = 9.3$ °C against F21T (*vide infra*), but more importantly an excellent selectivity over duplexes (illustrated by the selectivity value $^{FRET}S = 0.94$, indicating that the quadruplex stabilization is 94% maintained in the presence of a 50-fold excess of an unlabeled duplex-DNA competitor, *vide infra*). These results are important since they validate the proof-of-concept that synthetic G-quartets can be valuable quadruplex ligands.

Here, we decided to deeply rethink the synthesis of this compound in order to add a sidearm enabling surface-immobilization on graphene. We selected graphene because it is an emerging yet highly promising biosensor material, and used pyrene as the side arm, owing to its known ability to interact strongly with graphene in a non-covalent yet highly efficient manner (on the basis of both π-π stacking and hydrophobic interactions).[23] However, special care must be taken to avoid interactions between pyrene and G-quadruplexes, the pyrene being known as a duplex-DNA intercalator *per se*,[24] which would result in an alteration of the Tb.DOTASQ quadruplex-selectivity. Tb.Pyro-DOTASQ was thus designed to make guanines and pyrene diametrically opposed (Fig. 2), placing the pyrene as far as possible from the quadruplex-interacting region (*i.e.* the synthetic quartet). Tb.Pyro-DOTASQ thus harbors four guanine residues linked to a DOTA-type template bearing a quite original C-functionalization to allow for the introduction of the pyrene appendage far from the guanine moiety while maintaining the overall structure of the parent Tb.DOTASQ complex.

Synthesis of Tb.Pyro-DOTASQ

The synthetic access to Tb.Pyro-DOTASQ (Scheme 1) begins with the aminomethylcyclen **2**, synthesized according to a previously reported 5-step protocol from the commercially available triethylenetetramine (TETA, **1**).[25] A peptidic coupling between aminomethylcyclen **2** and the activated pyrene-acid conjugate, prepared from the commercially available 1-pyrenecarboxylic acid upon reaction with HOBt/EDCI, provided the desired Pyro-Cyclen derivative **3** with 41% overall yield. The synthetic pathway developed for the synthesis of Tb.DOTASQ was subsequently applied: the Pyro-DOTA-Et **4** was obtained after a reaction between the aforementioned Pyro-Cyclen **3** and four equivalents of ethylacetate bromide, delivering the desired compound **4** in 20% yield after purification by flash chromathography. This compound was subsequently reacted with an excess of ethylenediamine to afford Pyro-DOTA-NH2 **5** with 84% yield. Concurrently, the synthesis of the protected guanine arms was inspired by a previously reported 3-step protocol from the commercially available 2-amino-6-chloropurine:[26] the purine firstly reacts with the 6-methyl-bromohexanoate in presence of NaH, since the nucleophile substitution occurs specifically with the secondary amine (position 9); the obtained ester was subsequently saponified using LiOH, and finally the chloride of the purine (position 6) was substituted by a benzyloxy protecting group, to afford the protected guanine arms **6** in 14% chemical yield (three steps). The synthesis ends with a coupling reaction between Pyro-DOTA-NH2 **5** and guanine arms **6** under classical HOBt/EDCI conditions to afford, after a mild acidic treatment, the final Pyro-DOTASQ **7** in 10% yield over two steps. The chelation of the metal ($Tb(NO_3)_3.6H_2O$) by Pyro-DOTASQ completes the synthesis (MeOH/buffer pH 7.2 mixture). Pure analytical fractions of Tb.Pyro-DOTASQ were isolated by HPLC purification, with modest yields (6%) but high chemical purity.

Quadruplex-interacting Properties of Tb.Pyro-DOTASQ

The quadruplex affinity and selectivity of Tb.Pyro-DOTASQ was evaluated *via* fluorescence resonance energy transfer (FRET)-melting experiments (Fig. 3).[22] Briefly, this technique gives a quantification of the quadruplex apparent affinity of candidates through a temperature-induced modification of the FRET phenomenon that exists between two FRET partners; here, we used doubly labeled quadruplex-forming oligonucleotides, whose two extremities are labeled by fluorescein amidite (FAM or F) and carboxytetramethylrhodamine (TAMRA or T). The selected sequences used are FAM-$G_3(T_2AG_3)_3$-TAMRA, aka F21T, a 21-nt sequence that mimics the hu-

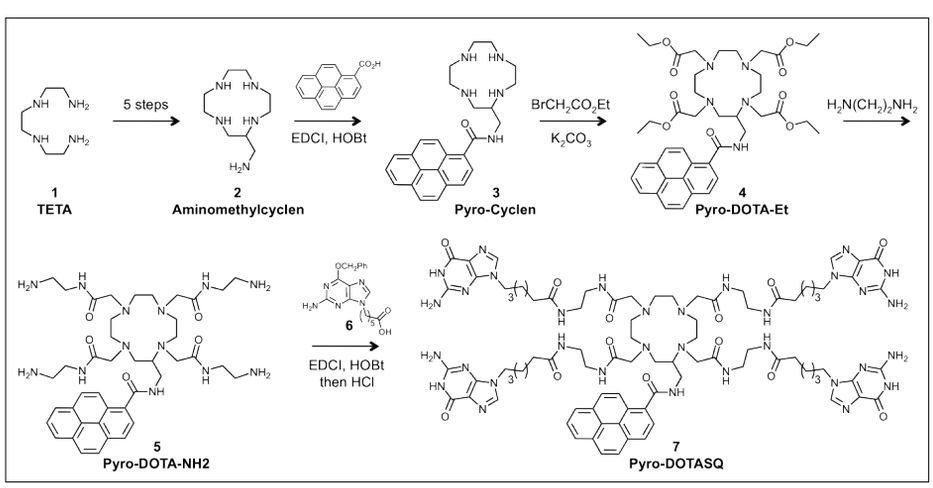

Scheme 1. Chemical synthesis of Pyro-DOTASQ.

man telomere, a standard in FRET-melting experiments,[22] and ds26, a self-complementary 26-nucleotide sequence that forms a duplex-DNA used as unlabelled competitor. Results seen in Fig. 3 indicate that the Tb.Pyro-DOTASQ is a good quadruplex binder (Fig. 3A), with properties that are even better than Tb.DOTASQ in terms of quadruplex affinity ($\Delta T_{1/2}$ = 15.3 *vs* 9.3 °C for Tb.Pyro-DOTASQ and Tb.DOTASQ, respectively) while slightly less quadruplex-selective (over duplex-DNA, ^{FRET}S = 0.69 *vs* 0.94 for Tb.Pyro-DOTASQ and Tb.DOTASQ, respectively). These results confirm that the presence of a bulky pyrene group within the structure of the complex does not impede its quadruplex interaction and could even be responsible for the even better quadruplex affinity of Tb.Pyro-DOTASQ, this bulky group acting as a steric hindrance that forces the four guanine arms to be on the same side of the DOTA template. They also indicate that the pyrene appendage does not interfere in the quadruplex binding process since it does not interact with oligonucleotides. To further assess this assumption, similar experiments were carried out with Pyro-DOTASQ, the demetalated analogue of Tb.Pyro-DOTASQ that should not be able to fold in its closed conformation. Under the same conditions, this compound imparts a very weak stabilization of F21T ($\Delta T_{1/2}$ = 2 °C, Fig. 3B), thus demonstrating that the presence of the metal is mandatory for the quadruplex affinity (reminiscent of the parent DOTASQ), and that the pyrene itself does not interact with DNA or, better put, the quadruplex interaction is driven by the quartet only. Altogether, these results make pyrene an ideal anchoring point for surface immobilization on graphene.

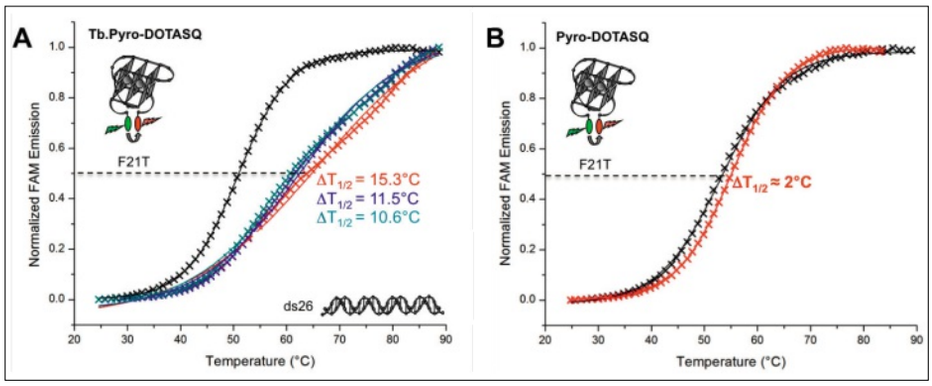

Fig. 3. Evaluation of the quadruplex affinity and selectivity of Tb.Pyro-DOTASQ *via* FRET-melting assay: experiments are carried out with 0.2 μM F21T in absence (black curve) or presence of 5 molar equivalents (1 μM, red curves) of Tb.Pyro-DOTASQ (**A**) or Pyro-DOTASQ (**B**) and increasing amounts of ds26 (**A**, 0, 3 and 10 μM, red, blue and green curves) in lithium cacodylate buffer pH 7.2 plus 10 mM LiCl/90 mM KCl.

Photophysical Properties of Tb.Pyro-DOTASQ

We thus decided to gain insight into the spectroscopic properties of this new ligand to assess whether the terbium could act as a conformational sensor. We indeed hypothesized that when the ligand is in contact with its quadruplex target, the exchange rate of the water molecule that completes the terbium coordination sphere is considerably slowed down (Fig. 2). This hampers the loss of accumulated energy by the complex through radiationless pathways, thus increasing the overall luminescence of the complex. It should be noted that terbium complexes usually require a sensitizing antenna to be luminescent, owing to the poor efficiency of direct metal excitation. Importantly, pyrene does not display suitable photophysical properties to act as a terbium sensitizer;[27] it was thus consciously selected here as an anchoring moiety because the quenching of its fluorescence emission upon interaction with graphene would have been incompatible with its efficient use as antenna. In our case, the antenna is not required since the guanines of the synthetic quartet can play that role intramolecularly, as demonstrated with the parent Tb.DOTASQ complex. The UV-Vis spectrum of the Tb.Pyro-DOTASQ indicates two maxima of light absorption at 245 and 343 nm, which correspond to the absorbance of the guanine and the pyrene, respectively. The fluorescence investigations were subsequently performed in the presence of an excess of quadruplex-DNA (up to 10 equiv. of c-kit, which corresponds to the quadruplex forming sequence found in the promoter region of the c-*KIT* oncogene, $CG_3CG_3CGCGAG_3AG_4$) in order to favor the Tb.Pyro-DOTASQ/quadruplex-DNA assembly in solution and thus, to favor the closed conformation of the TASQ. No typical luminescence signals (>500 nm) were observed under an excitation at 343 nm, indicating that pyrene does not act as sensitizing antenna. An irradiation was thus performed at 245 nm and satisfyingly leads to the appearance of the typical luminescence signals (three peaks of decreasing magnitude, at 545, 585 and 620 nm). This wavelength being not suited in the presence of an excess of DNA (screening effect from the bases in excess), the titration was repeated with an excitation at 308 nm, which corresponds to the valley between the absorbance of the bases and pyrene. As seen in Fig. 4A, a titration (addition of DNA on the terbium complex) carried out at this wavelength gives rise to the luminescence signals, along with a non-flat baseline (*vide infra*). Quite satisfyingly, the luminescence response depends on the DNA structure, being enhanced by the quadruplex c-kit and unchanged upon addition of the duplex ds26 (Fig. 4B). These results thus highlight that Tb.Pyro-DOTASQ is a valuable turn-on, luminescent sensor of quadruplexes.

Questioning the Actual Structure of the Tb.Pyro-DOTASQ Complex

We further investigated the luminescence properties of Tb.Pyro-DOTASQ *via* a 3D fluorescence analysis (excitation between 300 and 500 nm; emission between 500 and 600 nm), to better delineate which contributions are responsible for this emission pattern: as seen in Fig. 4C, while the overall fluorescence originates in three different contributions (arrows 2–4, *vide infra*), a unique origin is found for the luminescence signal at 545 nm (arrow 1): an excitation below 310 nm (highlighted by a white arrow, Fig. 4C) confirming that the nucleobases are the main terbium sensitizer. The overall fluorescence of the complex, which is responsible for the non-flat baseline seen in Fig. 4A, thus originates in the luminescence of the metal, either nucleobase-mediated (λ_{ex} < 310 nm, arrow 1) or direct (λ_{ex} = 460 nm, arrow 4), and the fluorescence of both the nucleobases (λ_{ex} < 310 nm, arrow 2) and the pyrene (λ_{ex} = 345 nm, arrow 3).

These results are interesting and allow the structure of Tb.Pyro-DOTASQ to be investigated, primarily the actual localization of the terbium ion: the luminescence of the complex mainly originates in the transfer of the fluorescence from the guanine, thus inferring that the metal may be close enough to the quartet to be efficiently sensitized. DOTA-type molecular cages are first-in-class metal chelating agents, providing thermodynamically and kinetically stable complexes; in light of the considerable wealth of data acquired over the years, our working hypothesis thus relies on a terbium chelation by the DOTA ring (in between the N4/O4 planes, hypothesis A, Fig. 5). However, G-quartets are known as efficient cation chelating agents as well;[5,28] therefore, an alternative hypothesis could be built on a terbium sequestration in between the quartet and the wreath of carbonyl groups found in the connect-

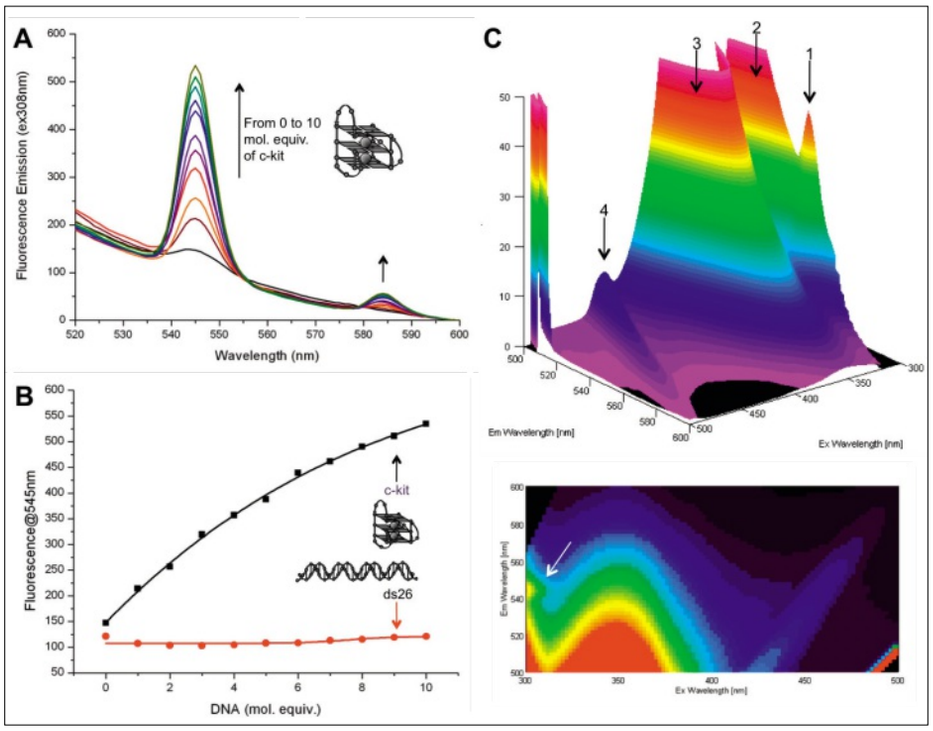

Fig. 4. DNA structure-selective luminescence response of Tb.Pyro-DOTASQ: experiments are carried out with 1 μM ligand without (black curve) or with increasing amounts of c-kit quadruplex (**A**, from 0 to 10 μM, from brown to green curves) in lithium cacodylate buffer pH 7.2 plus 10 mM LiCl/90 mM KCl. Comparison of results (**B**) for experiments carried out with c-kit (black curve) and ds26 (red curves). 3D fluorescence analysis of the Tb.Pyro-DOTASQ/c-kit complex (1:10), with λ_{ex} = 300–500 nm and λ_{em} = 500–600nm.

ing arms (between the G4/O4' planes, hypothesis B, Fig. 5). The fact that guanines sensitize terbium efficiently indicates that they are in close vicinity; this observation, along with the relative chemical fragility of the complex infers that, quite counter-intuitively, both hypotheses may be relevant. This is an important question, which must be addressed before proceeding any further in the implementation of the *in vitro* pull-down assay. Obtaining crystals suitable for X-ray crystallography would offer a golden way to adjudicate this scientific issue.

Conclusion

Herein we report on the design, the synthesis and the assessments of Tb.Pyro-DOTASQ as a nanotool for *in vitro* quadruplex interaction and detection. Thanks to its ability to fold into its closed conformation, the Tb.Pyro-DOTASQ complex interacts specifically with quadruplexes according to a nature-inspired approach. This quadruplex-promoted conformational switch triggers its affinity but also a luminescent response that allows for an easy and sensitive detection of quadruplexes in solution. The increase of the luminescent signals upon addition of quadruplex-DNA may originate from several factors: the closed conformation of the Tb.Pyro-DOTASQ is promoted by the presence of the quadruplex, which may contribute to bring the guanines closer to the metal and/or to freeze the movement of the water molecule that completes the coordination sphere of the metal (ninth position); alternatively, the Tb.Pyro-DOTASQ is in a close vicinity of the quadruplex-DNA that itself plays the role of terbium sensitizer through synthetic/native G-quartets interactions. This structure-specific energy transfer from the DNA matrix to the bound probe was indeed recently demonstrated with a quadruplex-selective fluorescent probe from the TASQ series.[14e] This transfer is made possible only by the biomimetic interaction between synthetic (ligand) and native (quadruplex) quartets, since this quite unique binding mode allows a physiologically cation (potassium) to be chelated in between the tetrad layers, the cation playing a central role in the efficiency of the energy transfer. The 2D/3D fluorescence results reported here indicate that the terbium is near the synthetic quartet when the TASQ interacts with quadruplexes, thereby implying that the G4/O4' terbium binding site may be privileged over the expected N4/O4 site. This would also account for the surprising lability of the metal complex; to tackle this issue, modification of the synthesis conditions are currently underway, notably using longer reaction times and higher temperatures to favor the 'thermodynamic' complex (*i.e.* the terbium in the N4/O4 binding site) over the 'kinetic' one (*i.e.* the terbium in the G4/O4' site). Firm structural investigations (notably X-ray crystallography analyses) are – and will also be systematically – required to unravel the exact nature of the resulting metal complexes. This provides a strong message that caution must be exercised in relying solely on standard chemical analysis methods when dealing with metal complexes with highly intricate structures.

Experimental Section

Synthetic Chemistry

NMR spectra were recorded on a Bruker DRX-300 AVANCE spectrometer at the *Pôle Chimie Moléculaire de l'Université de Bourgogne* (PACSMUB, Welience, UB-Filiale). HPLC was performed with an Ultimate 3000 Dionex UHPLC with an analytical Chromolith© SpeedROD (RP-18c, 50-4.6 mm) and semi-preparative Macherey-Nagel NUCLEODUR© (RP-18c, 10 × 250 mm, 5 μm) columns. Mass spectra were obtained with a Bruker Daltonics Ultraflex II spectrometer in the MALDI-TOF (Matrix Assisted Laser Desorption Ionization - Time of Flight)

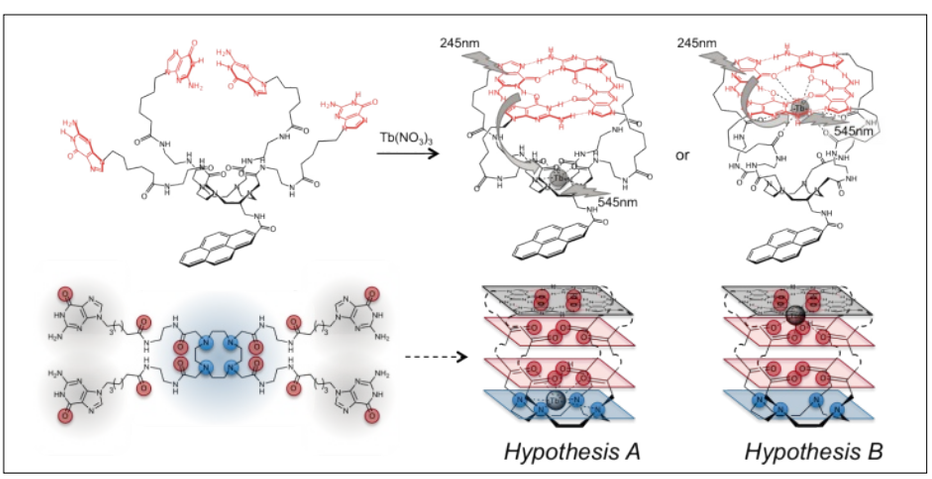

Fig. 5. Working hypotheses of the actual structure of Tb.Pyro-DOTASQ complex, primarily questioning the binding site of the terbium ion within the intricate Pyro-DOTASQ chelating agent.

reflectron mode using dithranol or 2,5-dihydroxybenzoic acid (DHB) as a matrix. Unless otherwise noted, all chemicals and solvents were of analytical reagent grade and used as received. Reactions were monitored by HPLC, UV/Vis and MALDI-TOF techniques. The synthesis of the aminomethylcyclen **2** from the commercially available TETA **1** and of the protected guanine **6** from the commercially available 2-amino-6-chloropurine have been performed as reported in refs. [25] and [26], respectively

Activation of 1-Pyrenecarboxylic Acid

To a solution of 1-pyrenecarboxylic acid (300 mg; 1.2 mmol; 1.0 equiv.) in CH_2Cl_2 (15 mL) were added HOBt (205 mg; 1.3 mmol; 1.1 equiv.) and EDCl.HCl (257 mg; 1.3 mmol; 1.1 equiv.). The yellow mixture was stirred at room temperature overnight, under N_2 atmosphere. CH_2Cl_2 (15 mL) was added to the formed heterogeneous mixture, until complete dissolution. The organic phase was washed with H_2O (2 × 15 mL), then dried over $MgSO_4$, filtrated and volatiles were removed under reduce pressure. The final compound was obtained as a bright yellow compound (435 mg; 1.2 mmol; 98% yield). *Characterizations*: ^{1}H NMR (300MHz, $CDCl_3$) δ (ppm): 7.54 (m, 3H), 8.21 (m, 8H), 9.03 (d, 1H), 9.18 (d, 8H), ^{13}C NMR {^{1}H} (75 MHz, $CDCl_3$) 108.7, 116.2, 120.7, 123.8, 124.0, 124.4, 124.9, 125.0, 127.0, 127.1, 127.4, 127.6, 128.9, 129.0, 129.3, 130.2, 130.9, 131.2, 131.4, 133.1, 136.4, 143.8, 163.2, MS (ESI): m/z = 386.091 $[M+Na]^+$ (69%); 749.193 $[2M+Na]^+$ (100%).

*Compound **3** (Pyro-Cyclen)*

Aminomethylcyclene (651 mg; 3.2 mmol; 2.2 equiv.) and the activated 1-pyrenecarboxylic acid prepared above (418 mg, 1.1 mmol, 1.0 equiv.) were dissolved in EtOH (18 mL). The mixture was stirred overnight at 80 °C. Volatiles were removed under vacuum and the obtained brown oil was taken up in CH_2Cl_2 (15 mL), then the desired compound was extracted with H_2O (3 × 10 mL). The aqueous phase (pH 10) was reduced under vacuum to deliver brown oil that was taken up in an 8M NaOH solution (10 mL) and then extracted again with CH_2Cl_2 (2 × 10 mL). The organic phase was dried over $MgSO_4$, filtered and volatiles were removed under reduce pressure. The compound **3** was obtained as brown oil (209 mg; 0.5 mmol; 43% yield). *Characterizations*: ^{1}H NMR (300MHz, $CDCl_3$) δ (ppm): 2.74 (broad, 19H), 3.66 (m, 2H), 8.13 (m, 9H), 8.61 (d, 1H), ^{13}C NMR {^{1}H} (75 MHz, $CDCl_3$) 41.9, 45.2, 46.0, 46.5, 46.6, 46.7, 46.8, 49.1, 54.7, 124.5, 124.7, 124.8, 125.8, 125.9, 126.5, 127.2, 127.3, 128.8, 130.9, 131.4, 131.5, 170.4, MS (ESI): m/z = 430.400 $[M+H]^+$ (100%); 452.400 $[M+Na]^+$ (25%).

*Compound **4** (Pyro-DOTA-Et)*

To a solution of compound **3** (159 mg; 0.4 mmol; 1.0 equiv.) in CH_3CN (11 mL), were added K_2CO_3 (409 mg; 3.0 mmol; 7.5 equiv.) and $BrCH_2CO_2Et$ (254 mg; 1.5 mmol; 4.0 equiv.). The pale orange mixture was stirred overnight at 45 °C. After cooling, K_2CO_3 was filtered off and the filtrate was concentrated under reduce pressure. The orange sticky solid was taken up with CH_2Cl_2 (15 mL), and this solution was washed with H_2O (2 × 10 mL). The organic phase was dried over $MgSO_4$, filtered and volatiles were removed under vacuum. The crude material was purified on an alumina column with CH_2Cl_2 and CH_2Cl_2 / MeOH (19:1) as eluents. Compound **4** was obtained as a yellow sticky solid (56 mg; 70 µmol; 20% yield). *Characterizations*: ^{1}H NMR (300MHz, $CDCl_3$) δ (ppm): 1.21 (m, 12H), 2.74 (broad, 14H), 3.01 (m, 3H), 3.39 (m, 8H), 4.11 (m, 8H), 7.21 (s, 1H), 8.14 (m, 8H), 8.63 (d, 1H), ^{13}C NMR {^{1}H} (75 MHz, $CDCl_3$) 14.4, 40.7, 51.2, 51.7, 52.7, 53.1, 53.2, 53.6, 55.5, 55.8, 56.3, 56.7, 57.3, 60.3, 60.5, 124.5, 124.8, 124.9, 125.7, 125.8, 126.3, 127.3, 128.6, 128.8, 130.8, 131.3, 131.4, 132.5, 170.3, 171.4, 171.7, 171.8, 171.9. MS (ESI): m/z = 688.400 $[M\text{-}CH_2CO_2Et+H]^+$ (100%); 710.400 $[M\text{-}CH_2CO_2Et+Na]^+$ (23%).

*Compound **5** (Pyro-DOTA-NH$_2$)*

Compound **4** (50 mg; 60 µmol; 1.0 equiv.) was dissolved in distilled ethylendiamine (6 mL). The solution was stirred at room temperature for 6 days, under inert atmosphere. Then, the ethylendiamine was co-evaporated with ACN (4 times). The compound **5** was precipitated in a small volume of ACN and filtered. The obtained solid was washed with small amounts of ACN (3 × 2mL) and dried to give the compound **5** as a brown solid (42 mg; 50 µmol; 84% yield). *Characterizations*: MS (ESI): m/z = 852.500 $[M+Na]^+$.

*Compound **7** (Pyro-DOTASQ)*

First step: To a solution of compound **5** (32 mg; 40 µmol; 1.0 equiv.) in DMF (5 mL) were added purine **6** (85 mg; 240 µmol; 6 equiv.), HOBt (37 mg; 240 µmol; 6 equiv.) and EDCI.HCl (46 mg; 240 µmol; 6 equiv.). The mixture was stirred for 4 days under inert atmosphere. Volatiles were removed under reduced pressure. Then, the crude material was dissolved in AcOEt (5 mL) and Et_2O was added until precipitation of the product. Once filtered, and dried under vacuum, the desired product was obtained as a pale brown solid (85 mg; 40 µmol; 98% yield). *Characterizations*: MS (MALDI-TOF): m/z = 2178.975 $[M+H]^+$. *Second step:* The previously prepared compound (81 mg; 40 µmol) was taken up in a solution of MeOH saturated by HCl (10 mL). The mixture was stirred at 20 °C for 1 h. The final product was precipitated by addition of diethyl ether (80 mL), and washed repeatedly with ether (20 mL). The crude material was purified by semi-preparative HPLC to afford compound **7** (7 mg; 4 µmol; 10% yield). *Characterizations*: ^{1}H NMR (300MHz, DMSO-d_6) δ (ppm): 1.24 (m, 8H), 1.51 (m, 8H), 1.79 (m, 8H), 2.05 (t, 8H), 2.40–4.20 (broad,), 3.06 (m, 16H), 4.06 (t, 16H), 7.11 (s, 8H), 7.40 (s, 4H), 7.86 (s, 4H), 8.33 (m, 9H), 8.95 (s, 4H), 11.49 (s, 4H), MS (MALDI-TOF) m/z = 645.064 $[M+3K]^+$ (100%); 1818.858 $[M+H]^+$ (61%); 1840.847 $[M+Na]^+$ (19%); 1856.809 $[M+K]^+$ (33%).

Tb.Pyro-DOTASQ

$Tb(NO_3)_3$ (1.9 mg; 4.2 µmol; 1.1 equiv.) was added to a 20 mM pH = 7.2 (1/1; 0.5 mL) MeOH/CacoLi solution of compound **7** (7.0 mg; 3.8 µmol; 1.0 equiv.). The mixture was stirred 4 days at 50 °C. After cooling, the final product was precipitated by addition of diethyl ether (25 mL), and washed repeatedly with ether (5 mL). Analytical fractions were purified by semi-preparative HPLC to afford the final compound (0.6 mg; 2.4 µmol; 6% yield) as white solid. *Characterizations*: MS (MALDI-TOF) m/z = 987.869 $[M]^{2+}$ (30%); 1818.868 $[M\text{-}Tb+H]^+$ (11%); 1974.773.835 $[M\text{-}2H]^+$ (100%).

Biophysical Investigations

UV-Vis experiments were carried out in 1 mL-quartz cuvettes (Starna) on a JASCO V630Bio spectrophotometer with a thermally controlled six-cell holder. All DNA/RNA samples were purchased from Eurogentec (Seraing, Belgium) in OligoGold® purity grade at 1000 nmol scale (purified by RP-HPLC). FRET-melting experiments were performed in a 96-well format using a Mx3005P real-time PCR machine (Agilent) equipped with a FAM filter (λ_{ex} = 492 nm; λ_{em} = 516 nm). The sequences (5'-to-3' direction) used herein were F21T FAM-d[$G_3(T_2AG_3)_3$]-TAMRA) and the unlabeled, self-complementary duplex-DNA used as competitor ds26 d[$CA_2TCG_2ATCGA_2T_2CGATC_2GAT_2G$]. The lyophilized DNA strands were firstly diluted in deionized water (18.2 MΩ.cm resistivity) as 500 µM solutions. F21T was prepared in a Caco.K buffer, comprised of 10 mM lithium cacodylate buffer (pH 7.2) plus 10 mM KCl / 90 mM LiCl, mixing 40 µL of the constitutive strand (500 µM) with 8 µL of a lithium cacodylate buffer solution (100 mM, pH 7.2), plus 8 µL of a KCl / LiCl solution (100 mM / 900 mM) and 24 µL of water. The duplex-DNA ds26 was prepared by mixing 40 µL of the constitutive strand (500 µM) with 16 µL of Caco.K buffer and 48µL of water. The final concentrations were theoretically 250 µM (F21T) or 125 µM (ds26): the actual

concentration of each solution was determined through a dilution to 1 µM theoretical concentration and UV spectral analysis at 260 nm (after 5 min at 90 °C) with the following molar extinction coefficient values: 268300 (F21T) and 506400 $M^{-1}.cm^{-1}$ (ds26). The higher-order DNA structures were folded *via* heating at 90 °C for 5 min and quick (F21T) or slow cooling (ds26, over 7 h) and then storage at 4 °C at least overnight.

FRET-melting Protocol

All the experiments were carried out with a total reaction volume of 100 µL with F21T (0.2 µM) in either Caco.K buffer (lithium cacodylate buffer (10 mM, pH 7.2) and KCl / LiCl (10 mM / 90 mM)) in absence or presence of increasing amounts of ds26 (3 and 10µM). Tb.Pyro-DOTASQ or Pyro-DOTASQ (stock solutions: 100 µM in DMSO) were added at 1 µM concentration. After a first equilibration step (25 °C, 30 s), a stepwise increase of 1 °C every 30 s for 65 cycles to reach 90 °C were performed, and measurements were made after each cycle. Final data were analyzed by using Excel (Microsoft) and OriginPro® 8 (OriginLab Corp. Northampton, MA, USA). The emission of FAM was normalized (0 to 1), and $T_{1/2}$ was defined as the temperature for which the normalized emission was 0.5; $\Delta T_{1/2}$ values were means of 2 to 4 experiments.

Fluorescence and UV-Vis Investigations

Fluorescence and UV-vis spectra were recorded on a JASCO FP8500 spectrofluorimeter and a JASCO V630Bio spectrophotometer, respectively, in a 10 mm pathlength quartz semi-micro cuvette (Starna). UV-Vis experiments were carried out with Tb.Pyro-DOTASQ (50 µM, 1 mM in DMSO, 50 µL) in 1 mL (final volume) of 10 mM lithium cacodylate buffer (pH 7.2) + 90 mM LiCl/10 mM KCl (from 200–1000 nm, bandwidth = 1.5 nm, scan speed = 400 $nm.mn^{-1}$). Fluorescent titrations were carried out in 1 mL (final volume) of 10 mM lithium cacodylate buffer (pH 7.2) + 90 mM LiCl/10 mM KCl, with Tb.Pyro-DOTASQ (1 µM, 1 mM in DMSO, 1 µL) alone or in presence of increasing amounts of DNA oligonucleotides (from 0 to 10 µM) being either c-kit (260 µM, 3.85 µL/molar equiv.) or ds26 (151 µM, 6.62 µL/molar equiv.). Spectra (λ_{ex} = 308 nm, λ_{em} = 520–660 nm, bandwidth = 5 nm, 0.5 s response, scan speed = 500 $nm.mn^{-1}$) were recorded 15 mn (at 25 °C) after each addition of the oligonucleotide.

Acknowledgements

This work was supported by the Centre National de la Recherche Scientifique (CNRS), Université de Bourgogne (uB) and Conseil Régional de Bourgogne (CRB) *via* 3MIM and PARI-SSTIC projects. The *Ministère de l'Enseignement Supérieur et de la Recherche* is acknowledged for Ph. D. grants (A. Laguerre and L. Stefan). F. Denat, F. Boschetti, C. Bernhard and S. Vuong are warmly thanked for their knowledge and help in macrocyclic chemistry.

Received: July 1, 2015

[1] a) J. D. Watson, F. H. C. Crick, *Nature* **1953**, *171*, 737; b) M. H. F. Wilkins, A. R. Stokes, H. R. Wilson, *Nature* **1953**, *171*, 738; c) R. E. Franklin, R. G. Gosling, *Nature* **1953**, *171*, 740.

[2] a) J. Marmur, P. Doty, *Nature* **1959**, *183*, 1427; b) N. Sueoka, J. Marmur, P. Doty, *Nature* **1959**, *183*, 1429.

[3] M. Gellert, M. N. Lipsett, D. R. Davis, *Proc. Natl. Acad. Sci. USA* **1962**, *48*, 2013.

[4] a) S. Sivakova, S. J. Rowan, *Chem. Soc. Rev.* **2005**, *34*, 9; b) J. L. Sessler, C. M. Lawrence, J. Jayawickramarajah, *Chem. Soc. Rev.* **2007**, *36*, 314; c) M. Fathalla, C. M. Lawrence, N. Zhang, J. L. Sessler, J. Jayawickramarajah, *Chem. Soc. Rev.* **2009**, *38*, 1608.

[5] a) J. T. Davis, *Angew. Chem. Int. Ed.* **2004**, *43*, 668; b) J. T. Davis, G. P. Spada, *Chem. Soc. Rev.* **2007**, *36*, 296; c) S. Lena, S. Masiero, S. Pierraccini, G. P. Spada, *Chem. Eur. J.* **2009**, *15*, 7792.

[6] a) N. Sreenivasachary, J.-M. Lehn, *Proc. Natl. Acad. Sci. USA* **2005**, *102*, 5938; b) E. Buhler, N. Sreenivasachary, S.-J. Candau, J.-M. Lehn, *J. Am. Chem. Soc.* **2007**, *129*, 10058; c) C. Arnal-Herault, A. Pasc, M. Michau, D. Cot, E. Petit, M. Barboiu, *Angew. Chem. Int. Ed*. **2007**, *46*, 8409.

[7] a) S. L. Forman, J. C. Fettinger, S. Pieraccini, G. Gottarelli, J. T. Davis, *J. Am. Chem. Soc.* **2000**, *122*, 4060; b) M. S. Kaucher, W. A. Harrell, J. T. Davis, *J. Am. Chem. Soc.* **2006**, *128*, 38; c) L. Ma, M. Melegari, M. Colombini, J. T. Davis, *J. Am. Chem. Soc*. **2008**, *130*, 2938; d) S. Bhosale, A. L. Sisson, N. Sakai, S. Matile, *Org. Biomol. Chem.* **2006**, *4*, 3031.

[8] a) M. Nikan, J. C. Sherman, *Angew. Chem. Int. Ed.* **2008**, *47*, 4900; b) M. Nikan, J. C. Sherman, *J. Org. Chem.* **2009**, *74*, 5211; c) M. Nikan, B. O. Patrick, J. C. Sherman, *ChemBioChem* **2012**, *13*, 1413.

[9] a) L. Stefan, F. Denat, D. Monchaud, *J. Am. Chem. Soc.* **2011**, *133*, 20405; b) S. Nakayama, K. Roelofs, V. T. Lee, H. O. Sintim, *Mol. Biosyst*. **2012**, *8*, 726; c) R. Haudecoeur, L. Stefan, D. Monchaud, *Chem. Eur. J.* **2013**, *19*, 12739; d) L. Stefan, D. Duret, N. Spinelli, E. defrancq, D. Monchaud, *Chem. Commun.* **2013**, *49*, 1500; e) B. T. Roembke, S. Nakayama, H. O. Sintim, *Methods* **2013**, *64*, 185.

[10] a) D. Sen, L. C. H. Poon, *Crit. Rev. Biochem. Mol. Biol.* **2011**, *46*, 478; b) S. K. Silverman, *Angew. Chem. Int. Ed.* **2010**, *49*, 7180; c) Y. Krishnan, F. C. Simmel, *Angew. Chem. Int. Ed*. **2011**, *50*, 3124; d) F. Wang, X. Liu, I. Willner, *Angew. Chem. Int. Ed.* **2015**, *54*, 1098.

[11] a) G. W. Collie, G. N. Parkinson, *Chem. Soc. Rev*. **2011**, *40*, 5867; b) P. Murat, S. Balasubramanian, *Curr. Opin. Gen. Dev.* **2014**, *25*, 22; c) M. L. Bochman, K. Paeschke, V. A. Zakian, *Nature Rev. Genet.* **2012**, *13*, 770; d) M. Tarsounas, M. Tijsterman, *J. Mol. Biol*. **2013**, *425*, 4782

[12] a) S. Burge, G. N. Parkinson, P. Hazel, A. K. Todd, S. Neidle, *Nucleic Acids Res.* **2006**, *34*, 5402; b) D. Yang, K. Okamoto, *Future Med. Chem.* **2010**, *2*, 619; c) A. T. Phan, *FEBS J.* **2010**, *277*, 1107

[13] a) J. L. Huppert, S. Balasubramanian, *Nucleic Acids Res.* **2005**, *33*, 2908; b) N. Maizels, L. T. Gray, *PLOS Genet.* **2013**, *9*, e1003468

[14] a) R. Rodriguez, K. M. Miller, J. V. Forment, C. R. Bradshaw, M. Nikan, S. Britton, T. Oelschlaegel, B. Xhemalce, S. Balasubramanian, S. P. Jackson, *Nature Chem. Biol.* **2012**, *8*, 301; b) G. Biffi, D. Tannahill, J. McCafferty and S. Balasubramanian, *Nature Chem*. **2013**, *5*, 182; c) G. Biffi, M. Di Antonio, D. Tannahill, S. Balasubramanian, *Nature Chem*. **2014**, *6*, 75; d) A. Henderson, Y. Wu, Y. C. Huang, E. A. Chavez, J. Platt, F. Brad, Johnson, R. M. Brosh Jr, D. Sen, P. M. Lansdorp, *Nucleic Acids Res.* **2014**, *42*, 860. e) A. Laguerre, K. Hukezalie, P. Winckler, F. Katranji, G. Chanteloup, M. Pirrotta, J.-M. Perrier-Cornet, J. M. Y. Wong, D. Monchaud, *J. Am. Chem. Soc.*, **2015**, *137*, 8521.

[15] a) A. De Cian, L. Lacroix, C. Douarre, N. Temime-Smaali, C. Trentesaux, J.-F. Riou, J.-L. Mergny, *Biochimie* **2008**, *90*, 131; b) Y. Xu, *Chem. Soc. Rev*. **2011**, *40*, 2719; c) S. Balasubramanian, L. H. Hurley, S. Neidle, *Nature Rev. Drug Discov*. **2011**, *10*, 261.

[16] a) B. Luke, J. Lingner, *EMBO J*., **2009**, *28*, 2503-2510; b) S. Schoeftner, M. A. Blasco, *EMBO J*., **2009**, *28*, 2323; c) A. Bugaut, S. Balasubramanian, *Nucleic Acids Res.* **2012**, *40*, 4727; d) P. Agarwala, S. Pandey, S. Maiti, *Org. Biomol. Chem.* **2015**, *13*, 5570.

[17] a) S. Müller, R. Rodriguez, *Expert Rev. Clin. Pharmacol.* **2014**, *7*, 663; b) S. Ohnmacht, S. Neidle, *Bioorg. Med. Chem. Lett*. **2014**, *24*, 2602.

[18] a) M. Di Antonio, R. l. Rodriguez, S. Balasubramanian, *Methods* **2012**, *57*, 84; b) R. Rodriguez, K. M. Miller, *Nature Rev. Genet.* **2014**, *15*, 783.

[19] L. Stefan, A. Guédin, S. Amrane, N. Smith, F. Denat, J.-L. Mergny, D. Monchaud, D. *Chem. Commun.* **2011**, *47*, 4992

[20] H.-J. Xu, L. Stefan, R. Haudecoeur, S. Vuong, P. Richard, F. Denat, J.-M. Barbe, C. P. Gros, D. Monchaud, *Org. Biomol. Chem.* **2012**, *10*, 5212;

[21] a) R. Haudecoeur, L. Stefan, F. Denat, D. Monchaud, D. *J. Am. Chem. Soc*. **2013**, *135*, 550; b) A. Laguerre, N. Desbois, L. Stefan, P. Richard, C. P. Gros, D. Monchaud, *ChemMedChem* **2014**, *9*, 2035; c) A. Laguerre, L. Stefan, M. Larrouy, D. Genest, J. Novotna, M. Pirrotta, D. Monchaud, *J. Am. Chem. Soc*. **2014**, *136*, 12406

[22] a) A. De Cian, L. Guittat, M. Kaiser, B. Saccà, S. Amrane, A. Bourdoncle, P. Alberti, M.-P. Teulade-Fichou, L. Lacroix, J.-L. Mergny, *Methods* **2007**, *42*, 183; b) D. Renciuk, J. Zhou, L. Beaurepaire, A. Guédin, A. Bourdoncle, J.-L. Mergny, *Methods* **2012**, *57*, 122.

[23] a) A. K. Geim, K. S. Novoselov, *Nature Mat.* **2007**, *6*, 183; b) M. J. Allen, V. C. Tung, R. B. Kaner, *Chem. Rev*. **2010**, *110*, 132; c) C.-H. Lu, J. Li, X.-L. Zhang, A.-X. Zheng , H.-H. Yang, X. Chen, G.-N. Chen, *Anal. Chem*. **2011**, *83*, 7276; d) R. K. Layek, A. K. Nandi, *Polymer* **2013**, *54*, 5087; e) C. B. CK, G. N. Lim, F. D'Souza, *Angew. Chem. Int. Ed.* **2015**, *54*, 5088.

[24] a) M. E. Ostergaard, P. J. Hrdlicka, *Chem. Soc. Rev.* **2011**, *40*, 5771; b) Y. N. Teo, E. T. Kool, *Chem. Rev.* **2012**, *112*, 4221.

[25] Y. Rousselin, N. Sok, F. Boschetti, R. Guilard, F. Denat *Eur. J. Org. Chem*. **2010**, 1688

[26] C. Schwergold, G. Depecker, C. Di Giorgio, N. Patino, F. Jossinet, B. Ehresmann, R. Terreux, D. Cabrol-Bass, R. Condom, *Tetrahedron* **2002**, *58*, 5675.

[27] a) A. Beeby, L. M. Bushby, D. Maffeo, J. A. Gareth Williams, *J. Chem. Soc., Perkin Trans. 2* **2000**, 1281; b) S. Faulkner, M.-C. Carrié, S. J. A. Pope, J. Squire, A. Beeby, P. G. Sammes *Dalton Trans.* **2004**, 1405.

[28] E. Galezowska, A. Gluszynska, B. Juskowiak, *J. Inorg. Biochem.* **2007**, *101*, 678.